




Radiocarbon dating of mangrove sediments to constrain Holocene relative sea-level change on Zanzibar in the southwest Indian Ocean

The Holocene
1–12
© The Author(s) 2015
Reprints and permissions:
sagepub.co.uk/journalsPermissions.nav
DOI: 10.1177/0959683615571422
hol.sagepub.com


Sarah A Woodroffe,¹ Antony J Long,¹ Paramita Punwong,^{2,3}
Katherine Selby,² Charlotte L Bryant⁴ and Rob Marchant⁵

Abstract

Mangrove sedimentary deposits are sensitive to changes in sea level and can be used to reconstruct mid- to late Holocene sea-level fluctuations in intermediate and far-field locations, distant to the former polar ice sheets. However, they can be difficult to date using ¹⁴C because mangrove sediment can contain mixtures of carbon of different ages. The two main potential causes of error are younger mangrove roots penetrating down through the sediment column and bioturbation by burrowing animals which moves carbon up and down the sediment column. Both processes may introduce carbon not representative of the age of deposition of the layer being dated. This study reports new ¹⁴C dates on organic concentrates (10–63 μm) from mangrove sediments from Makoba Bay on Zanzibar (Unguja) where previous bulk sediment ¹⁴C age–depth profiles contained inversions and were therefore less useful for relative sea-level (RSL) reconstruction. Dates on organic concentrates provide a more coherent sequence of ¹⁴C ages compared with those from bulk sediments. These new data provide an improved environmental history and mid- to late Holocene RSL record for this site. Our reconstructions show that RSL rose during the mid-Holocene and reached within –3.5 m of present by c. 7900 cal. yr BP. RSL slowed as it reached present at or shortly after c. 7000 cal. yr BP, with falling and/or stable RSL from c. 4400 cal. yr BP to present. We are not able to determine whether there was a RSL highstand above present on Zanzibar during the mid- to late Holocene. The RSL reconstruction agrees broadly with changes predicted by the ICE-5G geophysical model, which includes 4 m of ice equivalent sea-level rise between 7000 and 4000 cal. yr BP. Our new dating approach has the potential to provide improved chronologies with which to interpret sea level data from this and other mangrove environments.

Keywords

far field, mangroves, pollen, radiocarbon dating, sea level, southwest Indian Ocean

Received 28 January 2014; revised manuscript accepted 7 January 2015

Introduction

The spatial and vertical distribution of mangrove vegetation and their associated deposits are sensitive to changes in sea level (Scholl, 1964a, 1964b; Woodroffe et al., 1985). Because of their widespread occurrence in tropical environments, mangrove deposits therefore provide potentially important sources of ‘intermediate’ and ‘far-field’ sea-level observations (i.e. from sites that are distant from the significant effects of glacio-isostatic adjustment (GIA) found close to former ice sheets) and can provide valuable constraints on ice-equivalent sea-level changes (e.g. Milne and Mitrovica, 2008; Milne et al., 2005). However, the potential of mangroves is difficult to exploit because of challenges when using the radiocarbon dating method.

Previous studies of fossil mangrove sediments show that where mangrove environments are present for any length of time, younger mangrove roots will penetrate the older underlying sediments and introduce young carbon into bulk ¹⁴C samples, which will be young compared with the age of their original deposition (e.g. Grindrod and Rhodes, 1984; Schofield, 1977; Smith and Coleman, 1967; Woodroffe, 1981, 1988b, 1990). Because mangrove roots can penetrate up to 2 m into underlying sediments (Hutchings and Saenger, 1987), this can be a significant problem

when attempting to date mangrove sediment sequences. The problem is further compounded by bioturbation by a diverse fauna which may bring older organic material to the surface, increasing problems associated with obtaining reliable ages from these sediments.

We report a study designed to address the challenge of dating mangrove sediments by ¹⁴C AMS dating different size fractions of

¹Department of Geography, Durham University, UK

²Environment Department, University of York, UK

³Faculty of Environment and Resource Studies, Mahidol University, Thailand

⁴NERC Radiocarbon Facility (East Kilbride), Scottish Enterprise Technology Park, UK

⁵Environment Department, York Institute for Tropical Ecosystems (KITE), University of York, UK

Corresponding author:

Sarah A Woodroffe, Department of Geography, Durham University, Lower Mountjoy, South Road, Durham DH1 3LE, UK.

Email: s.a.woodroffe@durham.ac.uk

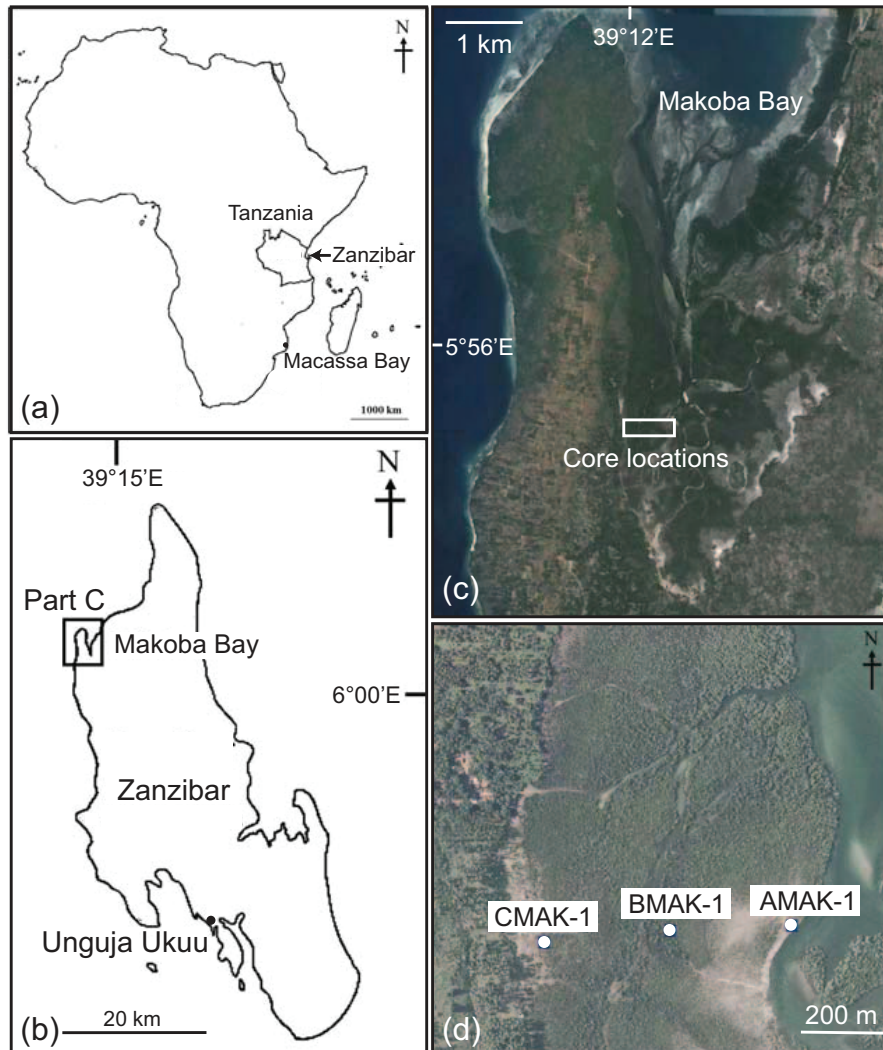


Figure 1. (a) Map showing the location of Zanzibar (Unguja) off the coast of Tanzania, (b) the position of Makoba Bay on the island of Zanzibar, (c) and (d) position of the sample cores in Makoba Bay.

organic matter extracted from material of mid- and late Holocene age collected from Zanzibar (Unguja), Tanzania. Pollen records from the study site show vertical trends that are ecologically sensible, stratigraphically coherent and apparently unaffected by significant bioturbation, yet bulk ^{14}C AMS ages on organic-rich sand and silt-rich mangrove deposits record age reversals that limit their utility for sea-level studies (Punwong et al., 2013b). Here, we date the 10–63 μm organic size fraction to produce nine ^{14}C AMS ages from two cores which previously had age reversals based on bulk AMS dates. We select this size fraction to exclude large organic fragments which are one potential source of young carbon, and also to increase the concentration of pollen in the samples. The results demonstrate more coherent age–depth relationships than by dating bulk sediments and enable us to compare resulting broad relative sea-level (RSL) reconstructions from this site with two GIA model predictions. Our study shows that ^{14}C AMS dating of the 10–63 μm organic size fraction from mangroves on Zanzibar provides good chronological control for reconstructing RSL change and ecosystem dynamics in this, and potentially other, mangrove environments.

Mangroves and RSL change

Mangroves are common on low latitude, tropical coasts and comprise physiologically adapted evergreen trees and shrubs that grow in the intertidal zone (Duke, 1992; Hogarth, 1999). They tolerate a salinity range that varies between fully marine water

(35‰) in the lowest intertidal area to freshwater in upstream rivers (Smith, 1992), depending on the gradient of the flood tide and freshwater runoff (Ball et al., 1988; Hogarth, 1999; Krauss et al., 2008). Their underlying sediments have the potential to provide important information on past vegetation change (Blasco et al., 1996; Woodroffe, 1990; Wooller et al., 2007) and, by inference, changes in RSL (e.g. Ellison, 1989, 2005; Engelhart et al., 2007; Horton et al., 2005; Woodroffe, 2009).

Previous work and study area

Our study site is Makoba Bay on the island of Zanzibar (Unguja), 40 km off the coast of Tanzania in the southwest Indian Ocean (Figure 1). The island sits within the 200 m isobath on the East African continental shelf (Arthurton et al., 1999). Previous studies from coastal locations in east and southeast Africa suggest RSL rose rapidly during the early Holocene in this region, reaching present by the mid-Holocene and rising to a highstand of +2.5 to +3 m above present mean sea level by 6000 cal. yr BP, before falling to present in the late Holocene (Compton, 2001, 2006; Jaritz et al., 1977; Katupotha, 1994; Norstrom et al., 2012; Ramsay and Cooper, 2002). The amplitude and timing of the RSL highstand is not well resolved in this region because of the large distances between field locations and the differing precision of the indicators used (Compton, 2001; Jaritz et al., 1977; Ramsay and Cooper, 2002). In contrast to these continental margin records, coral and sediment data from offshore coral, volcanic and

granitic islands in the southwest Indian Ocean suggest RSL only rose to close to present by c. 3000–2500 cal. yr BP with no mid- or late Holocene highstand (Braithwaite et al., 2000; Camoin et al., 1997, 2004; Woodroffe, in preparation; Zinke et al., 2003, 2005). This difference in the amplitude and timing of RSL changes may be because of the effects of hydro-isostatic loading and the associated ‘continental levering’ of the main African margin during the late Holocene, which was not experienced by off-shore islands that have narrow or no surrounding continental shelves and which, for this reason, are more reliable locations from where to reconstruct eustasy during the mid- and late Holocene (Milne and Mitrović, 2008).

The nature of mid- to late Holocene sea-level changes along the main East African margin after the initial peak of the highstand is also not well resolved. Studies which compare RSL data from sites up to ~1500 km apart along east and southwestern coasts often record multiple RSL fluctuations of up to ±2 m above present since c. 6000 cal. yr BP (Compton, 2001, 2006; Katupotha, 1994; Norstrom et al., 2012; Ramsay and Cooper, 2002). The driving mechanisms for these fluctuations are not known and may reflect local interactions between sediment accumulation and inundation during stable or slowly falling RSL (e.g. Woodroffe et al., 1985). An alternative explanation is that these fluctuations are an artefact of the methods and materials used in reconstructing past RSL as opposed to real changes in sea level. A general paucity of mid- and late Holocene RSL data from the east coast of Africa reflects in part difficulties in obtaining RSL information from tropical coastal environments, including mangroves which are extensive along this coastline yet difficult to reliably date.

Punwong et al. (2013b) detail previous litho- and biostratigraphic data from the Makoba Bay mangroves. Makoba Bay is a large macrotidal inlet to the northwest of Zanzibar with a tidal range of 4.3 m from lowest to highest astronomical tide (LAT and HAT; Admiralty Tide Tables, 2009). The upper intertidal areas are dissected by shallow tidal creeks and are vegetated by mature mangrove communities. The mangroves are broadly zoned with respect to elevation, with *Ceriops tagal* to the landward margins of main embayment, *Rhizophora mucronata* bordering tidal creeks within the mangrove belt and *Sonneratia alba* to the seaward. Seaward of the lowest mangroves are unvegetated tidal flats. Three sample cores of mangrove sediment were taken along a transect perpendicular to the coast, from the easterly (seaward) margin of the mangrove (core top elevation=0.60 m MTL, AMAK-1), from within the mangrove belt close to a tidal creek (core top elevation=0.45 m MTL, BMAK-1) and from the landward, westerly margin of the mangrove belt (core top elevation=1.51 m MTL, CMAK-1; Figure 1). The pollen content and chronologies provided by bulk ¹⁴C AMS dates from these three cores are shown in Figure 2 (see also Punwong et al., 2013b).

The lithologies of the two most seaward and lowest elevation cores (AMAK-1 and BMAK-1) comprise a lower unit of grey silt and sand which grade upwards into an organic sand that is overlain by mangrove peat containing woody roots and fine sand. The peat in each core is capped by a thin (<0.2 m thick) unit of sand that extends to the present surface. The pollen stratigraphies are dominated by *Bruguiera/Ceriops*, *Rhizophora mucronata* and *Sonneratia alba*, with lesser frequencies of *Avicennia marina* (Figure 2a and b). The stratigraphy of the most landward core (CMAK-1) comprises silt and sand at the base, which grade into an organic sand and then a sand towards the surface, with no intervening mangrove peat horizon (Figure 2c). Pollen was counted for only the top 1 m of this core and is dominated by *Rhizophora mucronata*, *Bruguiera/Ceriops* and *Sonneratia alba* (Figure 2c).

The basal sand and silt horizon in all three cores is dominated by *Rhizophora mucronata* pollen. *Rhizophora* spp. produce pollen in large quantities which is wind dispersed (Grindrod, 1985;

Hogarth, 2007). This likely explains its predominance throughout the sequence in all three fossil cores. *Bruguiera/Ceriops* and *Avicennia marina* pollen are also found in the basal sand and silt-rich sediments. Pollen from these mangrove species are not produced in such large numbers and are animal-dispersed (Hogarth, 2007), suggesting that mangrove was present on the site at the start of the sedimentary record in all three cores.

We have divided the pollen assemblages in each core into a series of zones which are present in part across all three cores. There is a basal *Rhizophora*-dominated assemblage (Zone 1) in BMAK-1, above which there is an assemblage also dominated by *Rhizophora*, but with a significant component of *Sonneratia alba* pollen in BMAK-1 and AMAK-1 (Zone 2). This returns to a *Rhizophora*-dominated assemblage up-core (Zone 3) followed by a small but significant increase in grasses and sedges towards the surface (Zone 4; Figure 2). The transition in the top c. 20 cm of the cores to sand may record a recent erosional surface, although in each core it contains mangrove pollen which conforms to the general trends in biostratigraphy. These changes in pollen assemblages up-core reflect vegetation changes that have been described from various locations around the Indo-west Pacific (Murray-Wallace and Woodroffe, 2014; Woodroffe, 1988a, 1990; Woodroffe et al., 1985).

Elsewhere in the Indo-west Pacific, a similar vegetation succession has been interpreted as being formed under an initial transgressive sequence caused by rising RSL (Zone 1) followed by a regressive sequence (Zones 2–4) associated with RSL fall or stability, where continuing sedimentation and mangrove succession choke out the mangrove swamp and allow the development of back-swamp grassland environments (Zone 4; Murray-Wallace and Woodroffe, 2014; Woodroffe, 1990; Woodroffe et al., 1985). Based on this model, Woodroffe et al. (1985) suggest that a peak in *Sonneratia* pollen seen in many mid-Holocene mangrove deposits should coincide with RSL reaching close to present for the first time during the Holocene. This is associated with mangrove expansion during the ‘big swamp phase’ seen in the South Alligator River and other estuaries in northern Australia and southeast Asia as RSL rise slowed during the mid-Holocene (Woodroffe, 1988a; Woodroffe et al., 1985).

Methods

¹⁴C AMS dating

The base of each core, the main stratigraphic boundaries and two within-unit levels were dated using bulk ¹⁴C AMS (Punwong et al., 2013; Table 1). These dates suggest that the deposits formed from the mid-Holocene onwards, but there are several age reversals (especially in BMAK-1 and CMAK-1) that make past RSL reconstruction difficult (Figure 2).

The original bulk sediment samples contained a mixture of wood fragments, organic remains and charcoal (Punwong et al., 2013b). For this study, we target eight levels adjacent to those previously sampled for bulk ¹⁴C AMS ages from cores AMAK-1 and BMAK-1 and a further near-surface level (3 cm deep in AMAK-1) for AMS ¹⁴C dating (Figure 2). We could not re-sample the exact same core depths that were used for bulk ¹⁴C AMS analysis because the sediment samples had been removed for previous analyses, but in all cases, we re-sampled within 4 cm of the original levels (Table 1).

We created an organic concentrate by firstly mixing the sediment with four times the sample volume of a mix of Na₄P₂O₄/NaOH to deflocculate any clays present within the sample, heated for 15 min in a water bath at 60°C and then centrifuged and removed the supernatant liquid. To remove carbonate material within the sample, we added 10% HCl to the sediment, heated to 85°C while stirring and then rinsed. Samples were then passed through 90, 63 and 10 μm sieves. We examined the different sample fractions

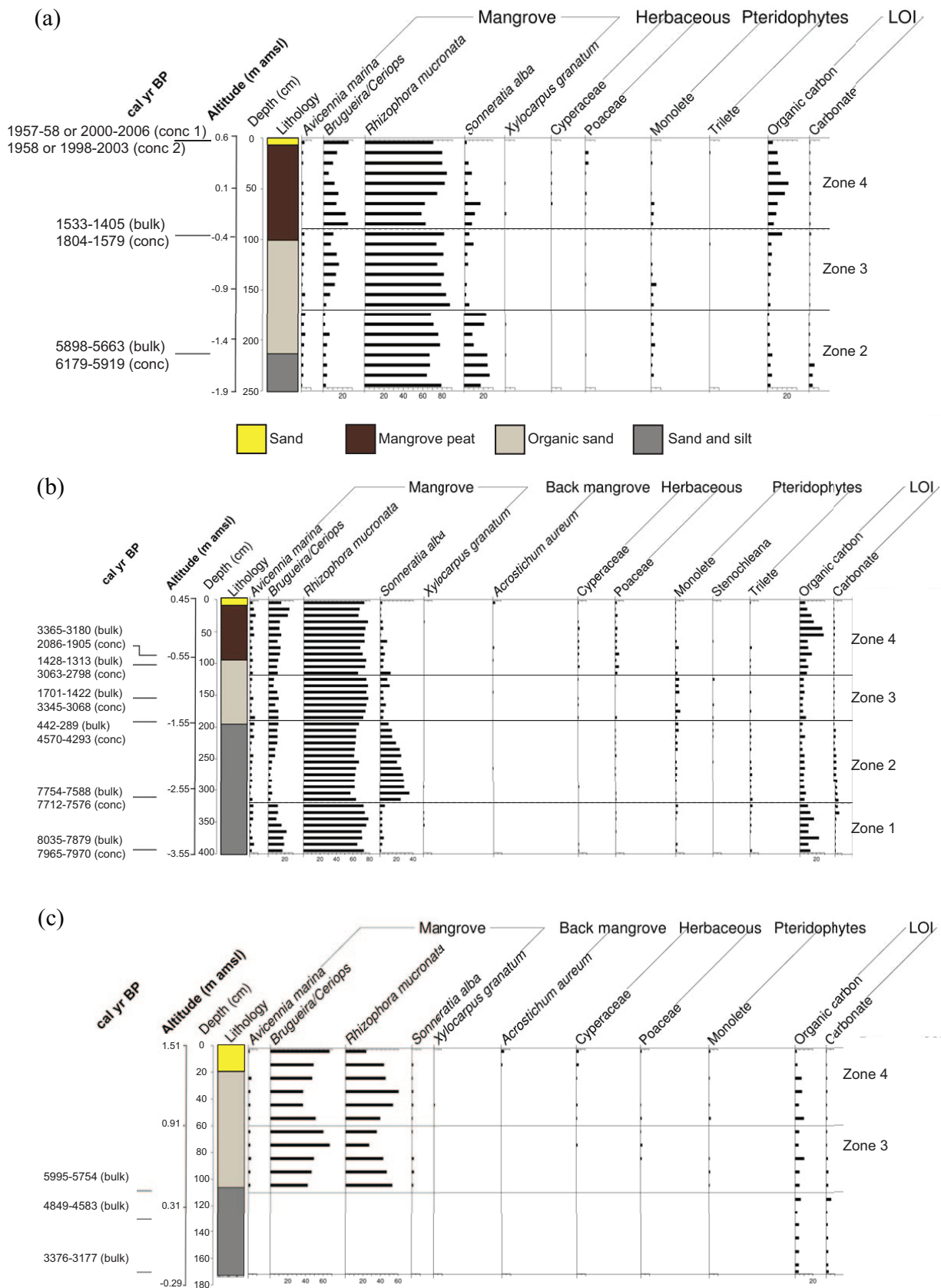


Figure 2. Pollen diagrams from (a) AMAK-I, (b) BMAK-I and (c) CMAK-I, showing core lithology, loss on ignition and the calibrated two sigma age ranges from bulk sediment and organic concentrate ^{14}C AMS dates (see Punwong et al., 2013b). Only species greater than 5% of the total pollen sum are shown.

under a light-transmitted microscope and chose the 10–63 μm fraction for dating to avoid large organic fragments that are one potential source of young carbon in mangrove sediment and because this fraction included mangrove pollen that is the material used for palaeoenvironmental reconstruction (Figure 3).

The dating of small organic size fractions has been previously identified as a way of concentrating pollen by excluding larger and smaller organic material (Li et al., 2014). However, in our case, the amount of pollen in the samples was very low (the pollen-based RSL reconstructions are based on counts of 150 grains;

Table 1. List of radiocarbon dates from bulk samples, organic concentrates and standards prepared with the organic concentrates.

Core number	Altitude (m m.s.l.)	Depth in core (cm)	Laboratory code	$\delta^{13}C_{VPDB}\text{‰}^a$	^{14}C yr BP	(2 σ) Calibrated age range yr BP	Indicative meaning (m MTL) (MTL to MHWST = 1.65 m)	RSL (m) based on range of modern mangroves (MTL to MHWST)
AMAK-I-3	0.42	3 (conc)	SUERC-44339	-26.8	% modern ^{14}C - 108.32 ± 0.48	^b 1957–1958 or 2000–2006	0.83 ± 0.83	-0.23 ± 0.83
			SUERC-41806	-26.7	% modern ^{14}C - 109.41 ± 0.50	^b 1958 or 1998–2003		
AMAK-I-98	-0.38	98 (bulk)	UBA-15378	-28.6	1615 ± 24	1533–1405	0.83 ± 0.83	-1.17 ± 0.83
	-0.34	94 (conc)	SUERC-44337	-25.9	1803 ± 36	1804–1579		
AMAK-I-212	-1.53	213 (bulk)	UBA-15379	-27.3	5078 ± 26	5898–5663	0.83 ± 0.83	-2.35 ± 0.83
	-1.52	212 (conc)	SUERC-44338	-24.3	5290 ± 38	6179–5919		
BMAK-I-97	-0.51	96 (bulk)	UBA-15380	-26.6	3111 ± 24	3365–3180	0.83 ± 0.83	-1.34 ± 0.83
	-0.52	97 (conc)	SUERC-41805	-26.4	2072 ± 35	2086–1905		
BMAK-I-106	-0.61	106 (bulk)	UBA-19415	-30.0	1543 ± 25	1428–1313	0.83 ± 0.83	-1.44 ± 0.83
	-0.62	107 (conc)	UERC-44340	-26.2	2864 ± 38	3063–2798		
BMAK-I-158	-1.13	158 (bulk)	UBA-16631	-33.0	1695 ± 50	1701–1422	0.83 ± 0.83	-2.00 ± 0.83
	-1.14	159 (conc)	SUERC-44341	-27.0	3053 ± 37	3345–3068		
BMAK-I-195	-1.50	195 (bulk)	UBA-15381	-28.0	309 ± 23	442–289	0.83 ± 0.83	-2.33 ± 0.83
	-1.51	196 (conc)	SUERC-42739	-20.0 ^c	4024 ± 40	4570–4293		
BMAK-I-320	-2.75	320 (bulk)	UBA-19416	-25.4	6878 ± 36	7754–7588	0.83 ± 0.83	-3.58 ± 0.83
	-2.76	321 (conc)	SUERC-44344	-26.3	6847 ± 39	7712–7576		
BMAK-I-396	-3.51	396 (bulk)	UBA-15382	-28.9	7202 ± 30	8035–7879	0.83 ± 0.83	-4.32 ± 0.83
	-3.49	394 (conc)	SUERC-44345	-27.0	7092 ± 38	7965–7970		
CMAK-I-107	0.44	107 (bulk)	UBA-15383	-26.1	5200 ± 35	5995–5754	0.83 ± 0.83	-0.39 ± 0.83
CMAK-I-130	0.21	130 (bulk)	UBA-16632	-23.8	4239 ± 37	4849–4583	0.83 ± 0.83	-0.62 ± 0.83
CMAK-I-172	-0.21	172 (bulk)	UBA-15384	-28.8	3117 ± 35	3376–3177	0.83 ± 0.83	-1.04 ± 0.83
Quality control materials:								
96H-Humin ^d 90 μ m	-	-	SUERC-41807	-28.0	3349 ± 35	-	-	-
Bituminous coal ^d 90 μ m	-	-	SUERC-41811	-21.8	Background % modern ^{14}C - 0.13 ± 0.01	-	-	-
IAEA C5 ^e 90 μ m	-	-	SUERC-41808	-24.8	11,706 ± 44	-	-	-
96H-Humin 10–63 μ m	-	-	SUERC-44346	-28.0	3410 ± 37	-	-	-
Bituminous coal 10–63 μ m	-	-	SUERC-44347	-23.2	Background % modern ^{14}C - 0.47 ± 0.01	-	-	-

RSL: relative sea level.

Calibrated ages from SHCal13 curve (Hogg et al., 2013) using the software OxCal v4.10 Bronk Ramsey (2009).

^aAn estimate of uncertainty in repeat combustion of homogenized sediment is c. ±0.5 per mil.^bCalibomb using SHZone3 and SHCal13 (Hogg et al., 2013; Hua et al., 2013). In both cases, the later date is the much more probable of the two age ranges (>90%) because the earlier date is on the rising, much steeper limb of the atmospheric ^{14}C curve.^cThe $^{13}C/^{12}C$ ratio for this sample was measured on the SUERC AMS during ^{14}C determination and used to model $\delta^{13}C$ values by comparison with the Craig (1957) $^{13}C/^{12}C$ value for PDB. This value is the most appropriate to normalize ^{14}C data to $\delta^{13}C_{VPDB}\text{‰} = -25$, but is not necessarily representative of the $\delta^{13}C$ in the original sample material.^dThe long-term in-house value for all pre-treatment types used at NRCF for bituminous coal is $0.21 \pm 0.12\%$ modern ^{14}C and for 96H-Humin is 3397 ± 42 ^{14}C yr BP.^eThe consensus value for IAEA-C5 is 11,780 ^{14}C yr BP (Rozanski et al., 1992).

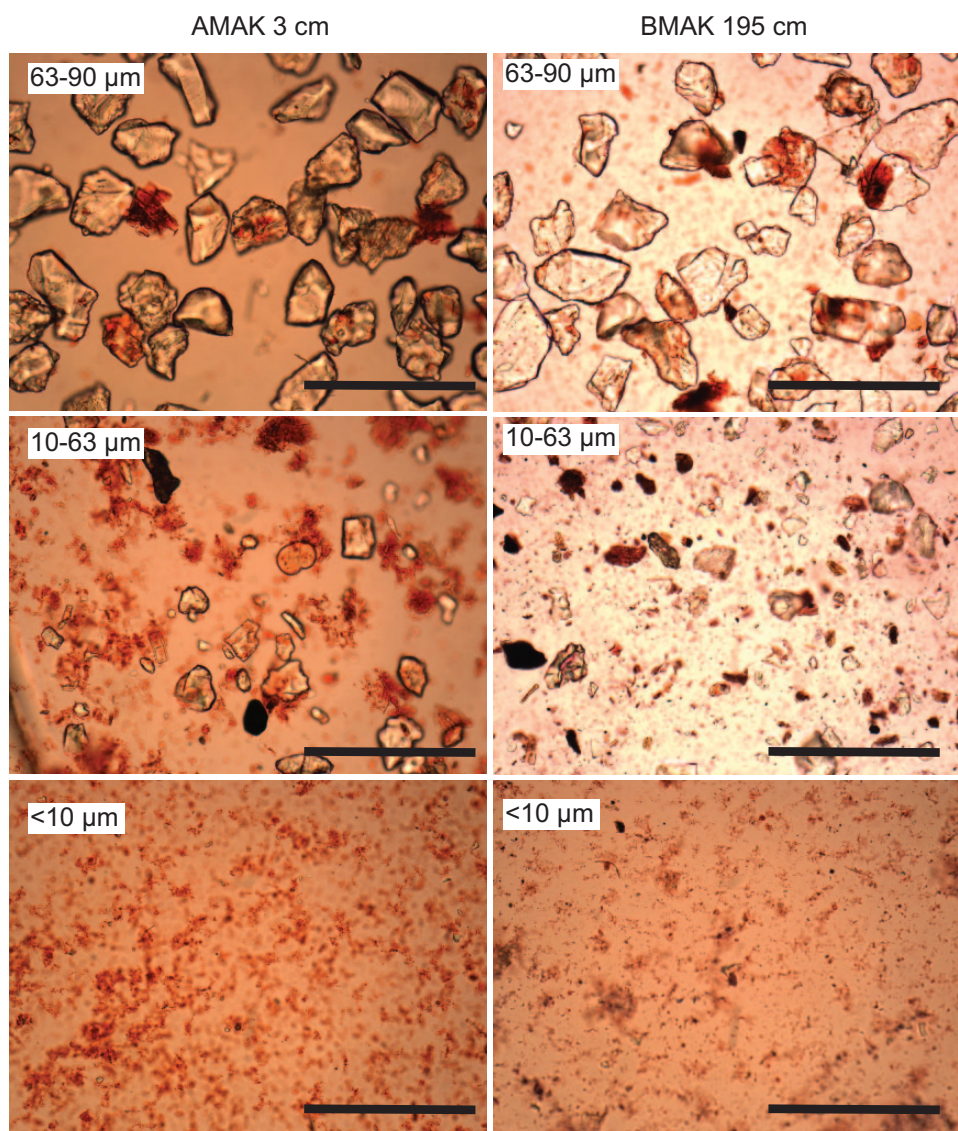


Figure 3. Photographs of three different sized sediment fractions in samples AMAK-I-3 and BMAK-I-195. These are representative of the type of material found at each sampled horizon in the cores. The scale bar on each is 100 μm . The dated sample in each case is the 10–63 μm fraction. The 63–90 μm fraction is dominated by inorganic particles and occasional pieces of plant material. The 10–63 μm fraction contains occasional pollen and smaller organic and inorganic material. The <10 μm fraction consists of a fine organic residue.

Punwong et al., 2013b). Therefore, the 10–63 μm fraction comprises sediment that is dominated by fine organic residue including pollen, rather than concentrated pollen only.

The organic concentrates were prepared to graphite at the NERC Radiocarbon Facility and analysed at the SUERC AMS Laboratory in East Kilbride. The $\delta^{13}\text{C}$ values were measured on a dual inlet stable isotope mass spectrometer (Thermo Fisher Delta V) and are representative of $\delta^{13}\text{C}$ in the original, pre-treated sample material. As part of this study, three process standards of known ^{14}C age and a background material (bituminous coal), which had undergone the same preparation process as the samples, were also analysed to identify any contamination by younger or older carbon. All dates are calibrated using the southern hemisphere calibration SHCal13 curve (Hogg et al., 2013) using the software OxCal v4.10 (Bronk Ramsey, 2009).

We reconstruct RSL at this location using two different methods. The first approach uses the vertical range of modern mangroves at Makoba Bay from MTL to MHWST as an indicative meaning for the fossil mangrove sediments. In the results, the mid-point in the modern distribution is plotted with the elevation error terms as the upper and lower limit of modern mangrove distribution. The second method is purely qualitative and

compares the pollen stratigraphy in the cores with those from other Indo-west Pacific locations that record mid-Holocene RSL rise followed by RSL stability or slow fall during the mid- to late Holocene (Grindrod, 1988; Woodroffe, 1990; Woodroffe et al., 1985). This enables broad interpretation of RSL changes but not quantitative reconstructions.

Results

Dating

The new radiocarbon dates range from the mid- to late Holocene (Table 1). The processed standards are within the 2σ confidence limits of expected values, and the background sample is in good agreement with the range of values previously obtained at the NERC Radiocarbon Facility (Table 1). We are confident that the preparation procedure has not introduced contamination into the samples.

Comparison of bulk and organic concentrate ^{14}C ages

We now compare the results from the existing bulk ^{14}C dates with the new organic concentrate samples from each core in turn. In

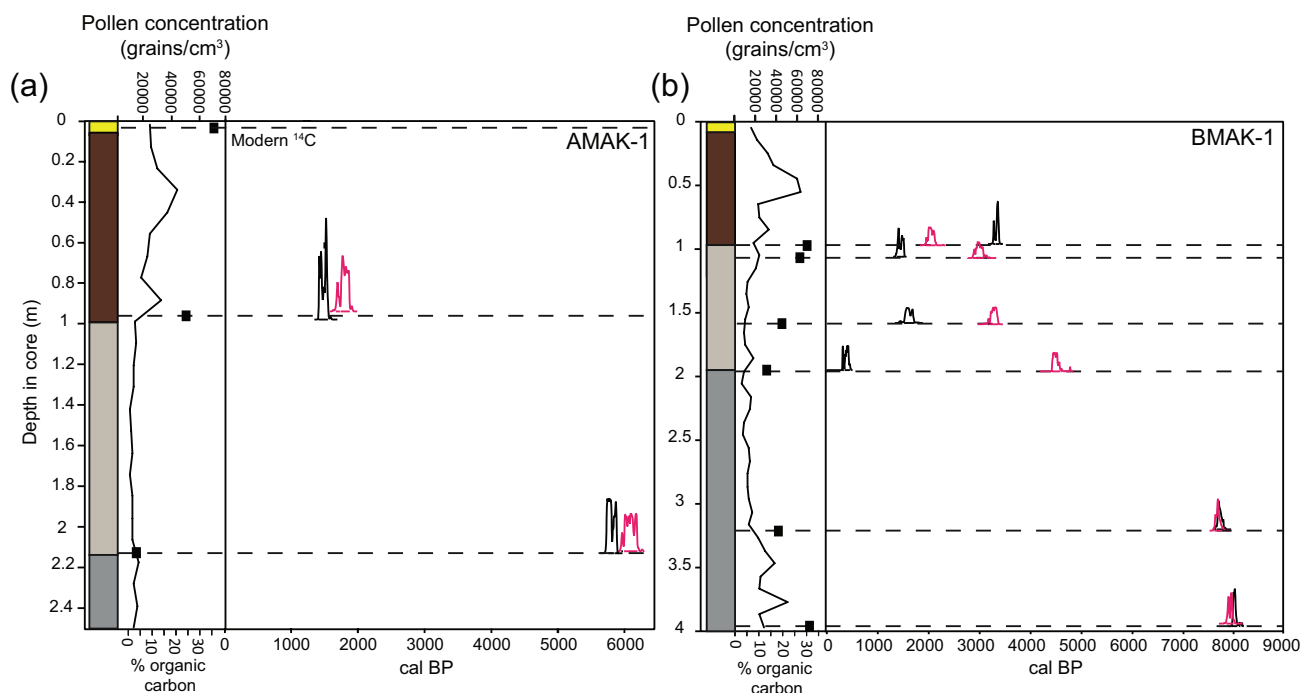


Figure 4. Age–depth plots for (a) AMAK-1 and (b) BMAK-1 showing the bulk (black) and organic concentrate (red) 2σ calibrated age ranges, along with the core lithology, % organic carbon (continuous line) through each core and the pollen concentration (black squares) at each horizon sampled for organic concentrate dating. The core lithology is summarized as grey – grey silt and sand, beige – organic sand, brown – mangrove peat containing wood fragments and fine sand, yellow – sand.

AMAK-1, a replicate pair of organic concentrate ages from 3 cm depth (AMAK-1-3) within the surface sandy layer yielded ages of AD 1957–1958 or AD 1998/2000–2003/2006. Two other organic concentrate ages from this core (AMAK-1-98 and AMAK-1-212) are each slightly older than the bulk ages 1–2 cm deeper, and their calibrated 2σ age errors do not overlap (Table 1, Figure 4a).

The bulk ^{14}C AMS chronology from BMAK-1 contains significant age reversals; an age of c. 300 cal. yr BP at 195 cm depth is overlain by material dating to c. 1500 and 3200 cal. yr BP at 158 and 96 cm, respectively (Figure 4b). Our organic concentrate ages provide a different but plausible chronology that is in sequence (Table 1). The paired bulk and organic concentrate ages on the two deepest samples (396–394 cm and 321–320 cm) agree, with their 2σ errors overlapping (Figure 4b). Different sized organic material has the same age in this part of the core. However, higher up the core where the organic content increases, there are significant, but not consistent, age differences between the two sample types. The largest discrepancy is at 196–195 cm (BMAK-1-195) where a bulk sediment sample yields a very young age and an organic concentrate sample an age of c. 4400 cal. yr BP. None of the other bulk samples from this core yield such a young age, so it is likely that this particular sample includes recent mangrove roots (which are not present in the 10–63 μm organic fraction). The uppermost three samples in BMAK-1 all show differences between the organic concentrate and bulk ages of between c. 1200 and 1600 cal. yr; in two cases, the organic concentrate ages are c. 1500 cal. yr older than the equivalent bulk ages (Table 1, Figure 4b).

$\delta^{13}\text{C}$ variations between bulk and organic concentrate samples

The measured $\delta^{13}\text{C}$ values of the dated bulk and organic concentrate samples show that the concentrate samples have more consistent $\delta^{13}\text{C}$ values and by inference sample fewer environments with different $\delta^{13}\text{C}$ values than the bulk samples (Table 1, Figure 5). The majority of bulk samples have more negative $\delta^{13}\text{C}$ values

than their corresponding concentrate samples, and there is a tendency towards more negative $\delta^{13}\text{C}$ values in the younger bulk samples where the organic content of the sample cores is highest. The $\delta^{13}\text{C}$ value of the anomalously young bulk age at BMAK-1-195 described above is not significantly different to those from other samples in the same horizon. The $\delta^{13}\text{C}$ value of this bulk sample does not indicate why it should have an anomalously young age.

Discussion

A comparison of bulk and organic concentrate ^{14}C AMS ages and $\delta^{13}\text{C}$ values

In all but one case, the organic concentrates from AMAK-1 and BMAK-1 are older than their equivalent bulk ^{14}C ages (Table 1). This implies that the bulk samples are primarily contaminated by young carbon that has been introduced to depth in the relevant profiles, which is sourced in the <10 or >63 μm size range. This is consistent with the hypothesis that younger mangrove roots penetrate older sediment and become incorporated into the sediment over time (Schofield, 1977; Smith and Coleman, 1967; Woodroffe, 1981, 1988b, 1990). The $\delta^{13}\text{C}$ values of the samples provide us further insight into the sources of carbon in the dated materials (Table 1 and Figure 5). A recent compilation of literature on measured $\delta^{13}\text{C}$ values from studies across the tropics on mangrove leaves shows a median $\delta^{13}\text{C}$ value of -28.0 with a 25–75% range from -29.4 to -27.0 , based on 495 measurements (Bouillon et al., 2008). In mangroves in Puerto Rico, leaves have more negative $\delta^{13}\text{C}$ values than stems and pneumatophores (Vane et al., 2013). The bulk samples from the most organic sections of cores AMAK-1 and BMAK-1 have $\delta^{13}\text{C}$ values within the range of the values for mangrove leaves while $\delta^{13}\text{C}$ values for the corresponding concentrate samples are less negative, but still within the range of C_3 plants (Figure 5). This is similar to the observations of Vane et al. (2013) who record less negative $\delta^{13}\text{C}$ values for mangrove sediments than for mangrove plant tissues.

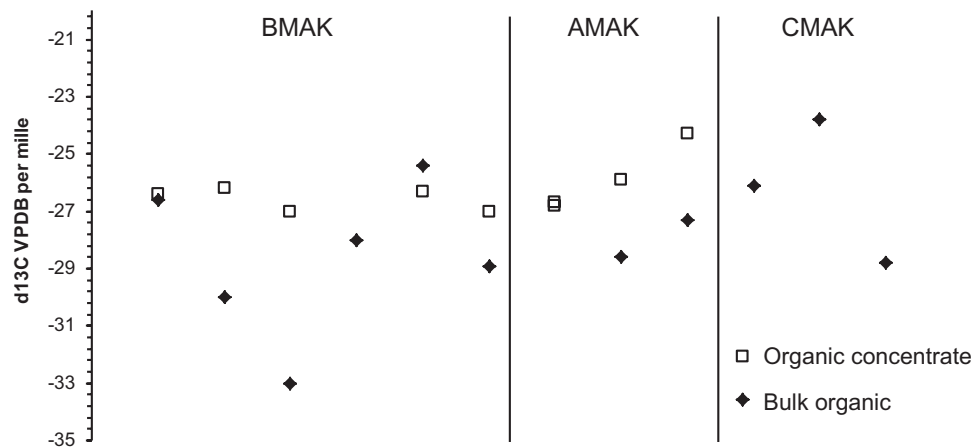


Figure 5. Plot of variations in $\delta^{13}\text{C}$ values of bulk and concentrate samples from the three cores from Makoba Bay.

Overall, the more negative $\delta^{13}\text{C}$ values of the bulk samples (−25.4‰ to −33‰, Figure 5) compared with the concentrates (−24.3‰ to −27‰, Figure 5) suggests that organic material, probably derived from younger mangrove plant tissues, is present in the bulk samples but not in the concentrates and is responsible for the younger ages of the bulk samples.

The one exception to this pattern is the bulk sample from the base of the organic-rich mangrove deposit in BMAK-1 (BMAK-1-97), which is older than the adjacent organic concentrate sample. The $\delta^{13}\text{C}$ values for the bulk and concentrate samples from this horizon are outside of the range of values for modern mangrove leaves (−26.6 (bulk) and −26.4 (concentrate)), and therefore, this bulk age is likely not affected by younger mangrove material. The most likely explanation here is that there is reworked old carbon included in this bulk sample, probably derived from catchment inwash since the $\delta^{13}\text{C}$ value suggests that this carbon is still from a non-marine environment (Figure 5, Table 1).

Bioturbation by burrowing animals is a widely recognized process in mangrove environments (Grindrod and Rhodes, 1984; Hogarth, 2007; Hutchings and Saenger, 1987). We might expect the concentrate ages to be both older and younger than the bulk ages if bioturbation by burrowing animals was causing significant sediment mixing, as this would bring older carbon nearer to the surface as well as younger carbon to depth in the sediment column. It is difficult to test this hypothesis with our samples because the 10–63 μm fraction may be preferentially dominated by old carbon. However, it is unlikely that the 10–63 μm fraction would be the only source of old carbon if burrowing animals were causing significant sediment mixing.

The pollen stratigraphy for the two cores shows no evidence for significant reworking. This is also the case in many other studies of Holocene mangrove pollen from the Indo-west Pacific region (Ellison, 1989; Engelhart et al., 2007; Grindrod and Rhodes, 1984; Woodroffe et al., 1985). However, our sampling resolution means we cannot wholly dismiss the influence of bioturbation by burrowing animals. Fiddler crabs (*Uca* spp.), that are present today in large numbers across the upper intertidal environment at Makoba Bay, typically burrow to depths of less than 30 cm (Qureshi and Saher, 2012). Based on our near-surface pollen concentrate date in BMAK-1, this suggests a potential mixing zone equivalent to 100–150 years in mangrove sediments which are continually accreting. If sedimentation rates were slower in the past because of RSL stability or fall for instance, this zone would have a longer duration and vice versa. Over mid- to late Holocene timescales, despite the fact that RSL was close to present, the mixing zone is unlikely to be identified in pollen analyses or organic concentrate ^{14}C ages because of the coarseness of our sampling intervals. However it has the potential to

introduce centennial and decimeter-scale errors in ages which may propagate into any pollen-based RSL reconstructions.

A new chronology for mangrove development and RSL changes on Zanzibar

The new organic concentrate ages provide an improved chronology for mangrove and RSL change over the past c. 7900 cal. yr at Makoba Bay. The analysed sediment cores range from 1.8 to 4 m in length and are organic-rich. They are therefore likely to have undergone post-depositional compaction. Using a vertical range of modern mangroves to reconstruct RSL suggests continual late Holocene RSL rise, but with large vertical uncertainties (Figure 6 and Table 1). This may seem surprising given Zanzibar's proximity to the main East African coastline, where mid- to late Holocene sea-level highstands are recorded up to +2.5 to +3 m above present (Compton, 2001; Jaritz et al., 1977; Katupotha, 1994; Norstrom et al., 2012; Ramsay and Cooper, 2002). Because we cannot quantify and correct for post-depositional compaction of the sediments from Makoba Bay, we are not confident that the quantitative reconstructions in Figure 6 accurately reflect changing RSL at this site during the mid- to late Holocene. Instead, we only make broad inferences about RSL based on the pollen data and new organic concentrate ages compared with changes in pollen assemblages found across the Indo-west Pacific region during the mid- to late Holocene (Figure 6). These broad inferences suggest that RSL was close to or above present during the mid- and late Holocene. We are unable to resolve whether the discrepancy between the two reconstructions is predominantly because of post-depositional compaction or other factors.

Mangrove sediments and their associated pollen are relatively good sea-level indicators during periods of rapid RSL rise, when waterlogging creates environments for mangroves to develop on formerly dryland surfaces where sediment bulk density is high and compaction is low (Murray-Wallace and Woodroffe, 2014). At Makoba Bay, these conditions existed around 7900 cal. yr BP, with the base of BMAK-1 recording a mangrove assemblage dominated by *Rhizophora mucronata* in a sand and silt substrate, when RSL first rose to within −3.5 m of present (Zone 1 in Figures 2 and 6). A comparable basal *Rhizophora*-dominated mangrove assemblage is also seen in cores from Unguja Ukuu, 50 km from Makoba Bay on the southwest coast of Zanzibar, where it is dated to around 7000 cal. yr BP (Punwong et al., 2013a). This level is our most robust sea-level indicator from the mid-Holocene because of the limited compaction at the core base. A subsequent peak in *Sonneratia alba* pollen in BMAK-1 above this horizon dates to c. 7000 cal. yr BP, with raised percentages of *Sonneratia alba* pollen between 7500 and 4400 cal. yr BP at

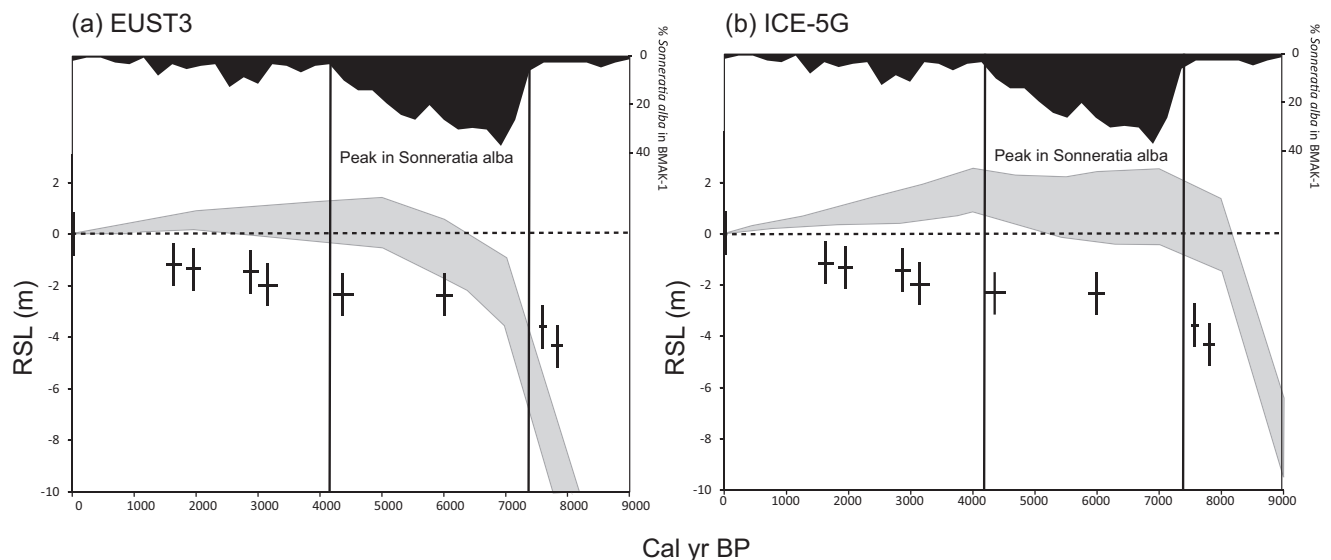


Figure 6. (a) RSL reconstructions from Makoba Bay using the modern elevation range of mangrove vegetation, % *Sonneratia alba* data from core BMAK-1 and RSL predictions from the EUST3 geophysical model (dark grey shading indicates the likely envelope of RSL change predicted by a series of geophysical model runs which sample a range of earth viscosity and lithospheric thickness parameters from lithosphere thickness 71–120 km, upper mantle viscosity between 0.1×10^{21} and 10^{21} Pa S and lower mantle viscosity between 10^{21} and 5×10^{22} Pa S). (b) RSL reconstructions and % *Sonneratia alba* data as before with RSL predictions from the ICE-5G geophysical model (dark grey shading indicates the likely envelope of RSL change predicted by the same series of model runs as in (a)) (Bradley et al., 2011; Peltier, 2004). RSL: relative sea level.

Makoba Bay (Zone 2 in Figures 2 and 6). As in many mangrove pollen records from the Indo-west Pacific region, we interpret the peak in *Sonneratia alba* as representing when RSL slowed as it first came close to present, representing the ‘big swamp phase’ of Woodroffe et al. (1985). Between c. 4000 cal. yr BP and present, the palynological evidence at Makoba Bay differs between cores, but a small increase in grassland pollen in both AMAK-1 and BMAK-1 suggests an increase in back-swamp environments under stable or slowly falling RSL (Zones 3 and 4 in Figure 2). A comparable small increase in grassland pollen in the late Holocene is also seen at Unguja Ukuu (Punwong et al., 2013a).

Accommodation space for sediment accretion would have been limited in the late Holocene as RSL was close to present, and near-surface sediments are more likely to be mixed as they would have lain within the reach of burrowing animals for several thousand years. The pollen zones at Makoba Bay agree closely with the model of mid- to late Holocene mangrove development during the initial RSL rise, RSL slow down and stability or RSL fall which is observed elsewhere in the Indo-west Pacific region (Grindrod, 1988; Woodroffe, 1988a, 1990; Woodroffe et al., 1985).

The mid-Holocene highstand

The timing of RSL first reaching close to present and the timing and amplitude of a mid-Holocene highstand on the East coast of Africa are not well resolved, partly because of the large distances between field sites and the varied RSL reconstruction methods used. However, most researchers agree that RSL was up to 2.5–3 m above present by 6000 cal. yr BP on the main coast, first rising above present sometime before this (Compton, 2001; Jaritz et al., 1977; Katupotha, 1994; Norstrom et al., 2012; Ramsay and Cooper, 2002). The coastal geomorphology of Zanzibar is dominated by fringing platforms and undercut cliffs 2–3 m above modern MHWST. Arthurton et al. (1999) interpret these as interglacial marine deposits dating from Marine Isotope Stage 5e, although dating evidence is limited. Seaward of these cliffs are beach ridge plains which extend up to 500 m inland from the backshore and are interpreted as being mid- to late Holocene in age (Arthurton et al., 1999). If this interpretation is correct, then these beach

ridge plains must have formed when RSL was close to or above present during the mid- and/or late Holocene, and when there was an abundant supply of sediment and accommodation space on the fringing platform, potentially under slowly falling RSL following a RSL highstand. We note that beach ridges can develop under falling, stable or even rising sea level depending on available sediment supply, but the geomorphology, combined with the biostratigraphic changes recorded in our sediment cores, is suggestive of either RSL stability or slow fall during the mid- to late Holocene. It is significant here that mangroves do not readily preserve evidence of falling RSL. This is because in tropical environments, former intertidal sediments which are no longer tidally flooded will oxidize and degrade over time (Murray-Wallace and Woodroffe, 2014). For this reason, it is possible that upper intertidal mangroves which may have formed under higher than present sea level have been eroded since the mid-Holocene. In this respect, we note also that the pollen zones in the cores from Makoba Bay are characteristic of both RSL stability and highstand situations in the mid- to late Holocene (Woodroffe, 1988a).

The wide distribution of mangrove pollen from different species across modern mangrove environments means that within-mangrove elevation changes are not readily reconstructed in the fossil record (Punwong et al., 2013b). However, it is interesting to note that the highest organic carbon values are found in the top ~1 m of AMAK-1 and BMAK-1 at Makoba Bay, which is dated to after c. 2900 cal. yr BP when RSL was likely stable or slowly falling. It is possible that compaction of the lower part of the sequence allowed renewed mangrove growth during this phase, which coincides with a small second peak in *Sonneratia alba* at similar levels in the two cores (Figure 2), and is also seen at Unguja Ukuu to the southeast of the island (Punwong et al., 2013a).

The evidence from this study suggests RSL rose rapidly to reach present c. 7900 cal. yr BP, after which RSL slowed as recorded by a peak in *Sonneratia alba* pollen at Makoba Bay (c. 7500–4400 cal. yr BP). This pattern agrees broadly with regional evidence from the main coast of East Africa of a mid- to late Holocene RSL highstand followed by a late Holocene RSL fall. However, despite improving the chronology of the sample cores by dating the fine organic fraction of these mangrove deposits, we

cannot quantitatively reconstruct the height of any mid- to late Holocene highstand because of the unknown effects of post-depositional compaction and the poor vertical resolution of mangrove pollen as a sea-level indicator in the macrotidal environment of Makoba Bay.

Comparison to geophysical model predictions for Zanzibar

RSL data from far-field locations such as Zanzibar can provide constraints on the magnitude and timing of mid- and late Holocene ice sheet melt, as well as on the effects of continental levering caused by water loading of continental shelves, equatorial siphoning whereby ocean water is redistributed to the collapsing forebulges of the former ice sheets and changes in earth rotation associated with mass transfer between ice sheets and the ocean (Milne and Mitrovica, 2008).

We compare our new broad estimates of mid- to late Holocene RSL with modelled RSL curves developed from the GIA models ICE-5G and EUST3 (Bradley et al., 2011; Peltier, 2004) for both our field site on Zanzibar and the location of the nearest Holocene RSL reconstruction on the main East African continental margin (Macassa Bay, Mozambique (Figure 1, data not shown); Norstrom et al., 2012). ICE-5G assumes that global ice melt ceased c. 4000 cal. yr BP, with 4 m of ice-equivalent sea-level rise between 7000 and 4000 cal. yr BP, while EUST3 has a longer global ice melting tail in the late Holocene which equates to 6 m ice-equivalent sea-level rise between 7000 and 2000 cal. yr BP. The details of the earth model parameters used in the GIA model runs are found in the caption for Figure 6.

Because of the poor vertical precision of the mangrove-based reconstructions from Makoba Bay, it is not possible to conclusively rule in or out a highstand, or indeed the potential magnitude of any highstand in this study. It is interesting to note, however, that within the range of ICE-5G and EUST3 model predictions, the majority of solutions include a RSL highstand, of up to c. 2.5 m for ICE-5G and c. 1.2 m for EUST3 (Figure 6). Despite the lack of sedimentary evidence to rule in or out at highstand, we can, however, compare the timing of the reconstructed mid-Holocene RSL rise and RSL slow down at Makoba Bay with the model predictions for the same location. The timing of RSL stability by around 7000 cal. yr BP (BMAK-1) and certainly before 6000 cal. yr BP (AMAK-1) as recorded by peaks in *Sonneratia alba* pollen is in broad agreement with the timing of RSL slow down predicted by ICE-5G (Figure 6b). By contrast, the maximum highstand in the EUST3 predictions comes later (c. 5000 cal. yr BP, Figure 6a) during the latter part of the *Sonneratia* peak. However, a peak in *Sonneratia* is only a broad indicator of RSL stability, and therefore, we cannot rule out the possibility that the EUST3 predictions also fit the available data. Our interpretation of a slow RSL fall or RSL stability from c. 4400 cal. yr BP onwards is in agreement with both the ICE-5G and EUST3 predictions. Overall, from the observational data available at Makoba Bay, we are not able to differentiate between the two different global ice sheet melt scenarios presented in ICE-5G and EUST3.

RSL predictions for Macassa Bay in Mozambique, on the main East African continental margin, show a similar magnitude maximum highstand elevation to those produced for Makoba Bay (c. 2.6 m for ICE-5G and c. 1.5 m for EUST3 at Macassa Bay (data not shown) compared with 2.5 m for ICE-5G and c. 1.2 m for EUST3 at Makoba Bay). Observational evidence suggests that there was a mid- to late Holocene highstand in this location, but its magnitude is not well constrained (Norstrom et al., 2012). Comparison between predicted highstand elevations at the East African continental margin and Zanzibar suggests that the location of Zanzibar, only 40 km offshore from the main coast of Tanzania, is not sufficiently distant from the continental margin to

be differentially affected by continental levering through the Holocene. In other locations, such as the central Great Barrier Reef shelf of Australia, lower magnitude highstands are predicted with increasing distance from the continental margin (Nakada and Lambeck, 1989). This modelling adds further weight to the argument that a lack of evidence for a highstand in the sediments from Makoba Bay is probably because of compaction and/or oxidation and degradation of the mangrove sediments over time and not because RSL was continually rising through the mid- to late Holocene in this location.

Conclusion

The results of this study demonstrate that the ^{14}C AMS dating of organic concentrates from mangrove environments is a potentially important new way of developing chronologies of RSL change from tropical mangrove settings in Zanzibar and other tropical locations where mangroves exist. Our conclusions are as follows:

- ^{14}C AMS dates of bulk mangrove sediment are often unreliable for reconstructing RSL because the sediment contains mixtures of carbon from different sources, which may include material not representative of the timing of deposition of the layer being dated.
- Previously published bulk sediment ^{14}C ages from Makoba Bay (Zanzibar) suggest mangrove sediment accumulated from c. 7900 cal. yr BP onwards. However, bulk sediment age–depth profiles contain inversions and are not useable for RSL reconstruction.
- AMS ^{14}C dates on organic concentrates (10–63 μm) from the same sample cores provide a more coherent sequence of ages compared with those developed from bulk sediments, with additional information on the sources of carbon in the sediments being provided by $\delta^{13}\text{C}$ data.
- The new ages are generally older than the bulk equivalents and provide a more continuous spread of data across the mid- and late Holocene.
- RSL reached within -3.5m of present by c. 7900 cal. yr BP, continued to rise and reached present at or after c. 7000 cal. yr BP. We are unable to reconstruct whether RSL rose above present in the mid-Holocene, or the height of any RSL highstand from our data because of the effects of post-depositional compaction and the broad vertical range of different mangrove species.
- The broad ecological changes recorded by the pollen data accord with previous studies of mangrove dynamics in locations within the Indo-west Pacific that have experienced a period of rapid RSL rise in the mid-Holocene, followed by RSL slow down and either stability or slow RSL fall in the late Holocene.
- Our most reliable RSL data are from the core bases, where compaction is least significant. The timing of the mid-Holocene RSL slow down and stability or highstand peak agrees most closely to predictions of the ICE-5G geophysical model, which includes 4 m of ice-equivalent sea-level rise between 7000 and 4000 cal. yr BP. However, we cannot totally rule out the alternative EUST3 geophysical model melt history, which includes a larger late Holocene melting tail. All of the ICE-5G and most of the EUST3 modelled RSL curves for Makoba Bay include a highstand, and it is very likely that the sediments have been compacted or degraded over time, which means they fail to record a mid- to late Holocene sea-level highstand in this location.
- The new approach presented here has the potential to provide improved chronologies with which to interpret sea-level data from other mangrove environments.

Acknowledgements

The original relative sea-level reconstructions and bulk AMS ^{14}C dating was undertaken as a part of Paramita Punwong's PhD thesis from the University of York. We are grateful to Glenn Milne for providing GIA model predictions. We also thank Maria Gehrels for help in the preparation of the samples used for dating. This paper is a contribution to PALSEA2, IGCP588 and the INQUA Commission on Coastal and Marine Processes. Colin Woodroffe and another reviewer provided helpful and constructive comments on the paper.

Funding

Punwong was supported by The Royal Thai Government Scholarship, BIEA, WWF-Tz, and NMK. Funding for the radiocarbon dates on the organic concentrates was received through NERC Radiocarbon Facility Allocation 1608.0312.

References

- Admiralty Tide Tables (2009) *NP203 Admiralty Tide Tables (ATT) Volume 3, Indian Ocean and South China Sea (including Tidal Stream Tables)*. Taunton: Hydrographer of the Navy.
- Arthurton RS, Brampton AH, Kaaya CZ et al. (1999) Late quaternary coastal stratigraphy on a platform-fringed tropical coast – A case study from Zanzibar, Tanzania. *Journal of Coastal Research* 15: 635–644.
- Ball MC, Cowan IR and Farquhar GD (1988) Maintenance of leaf temperature and the optimization of carbon gain in relation to water-loss in a tropical mangrove forest. *Australian Journal of Plant Physiology* 15: 263–276.
- Blasco F, Saenger P and Janodet E (1996) Mangroves as indicators of coastal change. *Catena* 27: 167–178.
- Bouillon S, Connolly RM and Lee SY (2008) Organic matter exchange and cycling in mangrove ecosystems: Recent insights from stable isotope studies. *Journal of Sea Research* 59: 44–58.
- Bradley SL, Milne GA, Shennan I et al. (2011) An improved glacial isostatic adjustment model for the British Isles. *Journal of Quaternary Science* 26: 541–552.
- Braithwaite CJR, Montaggioni LF, Camoin GF et al. (2000) Origins and development of Holocene coral reefs: A revisited model based on reef boreholes in the Seychelles, Indian Ocean. *International Journal of Earth Sciences* 89: 431–445.
- Bronk Ramsey C (2009) Bayesian analysis of radiocarbon dates. *Radiocarbon* 51: 337–360.
- Camoin GF, Colonna M, Montaggioni LF et al. (1997) Holocene sea level changes and reef development in the southwestern Indian Ocean. *Coral Reefs* 16: 247–259.
- Camoin GF, Montaggioni LF and Braithwaite CJR (2004) Late glacial to post glacial sea levels in the Western Indian Ocean. *Marine Geology* 206: 119–146.
- Compton JS (2001) Holocene sea-level fluctuations inferred from the evolution of depositional environments of the southern Langebaan Lagoon salt marsh, South Africa. *The Holocene* 11: 395–405.
- Compton JS (2006) The mid-Holocene sea-level highstand at Bogenfels Pan on the southwest coast of Namibia. *Quaternary Research* 66: 303–310.
- Craig H (1957) Isotopic standards for carbon and oxygen and correction factors for mass-spectrometric analysis of carbon dioxide. *Geochimica et Cosmochimica Acta* 12: 133–149.
- Duke NC (1992) Mangrove floristics and biogeography. In: Robertson AI and Alongi DM (eds) *Tropical Mangrove Ecosystems*. Washington, DC: American Geophysical Union, pp. 63–100.
- Ellison J (2005) Holocene palynology and sea-level change in two estuaries in Southern Irian Jaya. *Palaeogeography, Palaeoclimatology, Palaeoecology* 220: 291–309.
- Ellison JC (1989) Pollen analysis of mangrove sediments as a sea-level indicator – Assessment from Tongatapu, Tonga. *Palaeogeography, Palaeoclimatology, Palaeoecology* 74: 327–341.
- Engelhart SE, Horton BP, Roberts DH et al. (2007) Mangrove pollen of Indonesia and its suitability as a sea-level indicator. *Marine Geology* 242: 65–81.
- Grindrod J (1985) The palynology of mangroves on a prograded shore, Princess Charlotte Bay, North Queensland, Australia. *Journal of Biogeography* 12: 323–348.
- Grindrod J (1988) The palynology of Holocene mangrove and saltmarsh sediments, particularly in northern Australia. *Review of Palaeobotany and Palynology* 55: 229–245.
- Grindrod J and Rhodes EG (1984) Holocene sea-level history of a tropical estuary: Missionary Bay, North Queensland. In: Thom BG (ed.) *Coastal Geomorphology in Australia*. Sydney: Academic Press, pp. 151–178.
- Hogarth PJ (1999) *The Biology of Mangroves*. New York: Oxford University Press.
- Hogarth PJ (2007) *The Biology of Mangroves and Seagrasses*. Oxford: Oxford University Press.
- Hogg AG, Hua Q, Blackwell PG et al. (2013) SHCal13 southern hemisphere calibration, 0–50,000 years cal BP. *Radiocarbon* 55: 1889–1903.
- Horton BP, Gibbard PL, Milne GA et al. (2005) Holocene sea levels and palaeoenvironments, Malay-Thai Peninsula, southeast Asia. *The Holocene* 15: 1199–1213.
- Hua Q, Barbetti M and Rakowski AZ (2013) Atmospheric radiocarbon for the period 1950–2010. *Radiocarbon* 55: 2059–2072.
- Hutchings P and Saenger P (1987) *Ecology of Mangroves*. St Lucia: University of Queensland Press.
- Jaritz W, Ruder J and Schlenker B (1977) Das Quartär im küstengebiet vom Moçambique und seine schwermineralführung. *Geologisches Jahrbuch* Reihe B: 3–93.
- Katupotha J (1994) Geological significance of marine molluscan beds: Evidence from southern coastal zone of Sri Lanka. *Journal of the National Science Council of Sri Lanka* 22: 157–187.
- Krauss KW, Lovelock CE, Mckee KL et al. (2008) Environmental drivers in mangrove establishment and early development: A review. *Aquatic Botany* 89: 105–127.
- Li C, Li Y and Burr GS (2014) Testing the accuracy of ^{14}C age data from pollen concentrates in the Yangtze delta, China. *Radiocarbon* 56: 1–7.
- Milne GA, Long AJ and Bassett SE (2005) Modelling Holocene relative sea-level observations from the Caribbean and South America. *Quaternary Science Reviews* 24: 1183–1202.
- Milne G and Mitrovica JX (2008) Searching for eustasy in deglacial sea-level histories. *Quaternary Science Reviews* 27: 2292–2302.
- Murray-Wallace CV and Woodroffe CD (2014) *Quaternary Sea-Level Changes: A Global Perspective*. Cambridge: Cambridge University Press.
- Nakada M and Lambeck K (1989) Late Pleistocene and Holocene sea-level change in the Australian region and mantle rheology. *Geophysical Journal* 96: 497–517.
- Norstrom E, Risberg J, Grondahl H et al. (2012) Coastal paleo-environment and sea-level change at Macassa Bay, southern Mozambique, since c 6600 cal BP. *Quaternary International* 260: 153–163.
- Peltier WR (2004) Global glacial isostasy and the surface of the ice-age earth: The ICE-5G (VM2) model and GRACE. *Annual Review of Earth and Planetary Sciences* 32: 111–149.
- Punwong P, Marchant R and Selby K (2013a) Holocene mangrove dynamics from Unguja Ukuu, Zanzibar. *Quaternary International* 298: 4–19.

- Punwong P, Marchant R and Selby K (2013b) Holocene mangrove dynamics in Makoba Bay, Zanzibar. *Palaeogeography, Palaeoclimatology, Palaeoecology* 379–380: 54–67.
- Qureshi NA and Saher NU (2012) Burrow morphology of three species of fiddler crab (*Uca*) along the coast of Pakistan. *Belgian Journal of Zoology* 142: 114–126.
- Ramsay PJ and Cooper JAG (2002) Late quaternary sea-level change in South Africa. *Quaternary Research* 57: 82–90.
- Rozanski K, Stichler W, Gonfiantini R et al. (1992) The IAEA C-14 intercomparison exercise 1990. *Radiocarbon* 34: 506–519.
- Schofield JC (1977) Late Holocene sea level, Gilbert and Ellice Islands, west central Pacific Ocean. *New Zealand Journal of Geology and Geophysics* 20: 503–529.
- Scholl DW (1964a) Recent sedimentary record in mangrove swamps and rise in sea level over the Southwestern Coast of Florida: Part 1. *Marine Geology* 1: 344–366.
- Scholl DW (1964b) Recent sedimentary record in mangrove swamps and rise in sea level over the Southwestern Coast of Florida: Part 2. *Marine Geology* 2: 343–364.
- Smith TJ (1992) Forest structure. In: Robertson AI and Alongi DM (eds) *Tropical Mangrove Ecosystems*. Washington, DC: American Geophysical Union, pp. 101–137.
- Smith WG and Coleman JM (1967) Recent submergence of Southern Florida – Discussion. *Geological Society of America Bulletin* 78: 1191–1194.
- Vane CH, Kim AW, Moss-Hayes V et al. (2013) Degradation of mangrove tissues by arboreal termites (*Nasutitermes acajutlae*) and their role in the mangrove C cycle (Puerto Rico): Chemical characterization and organic matter provenance using bulk delta C-13, C/N, alkaline CuO oxidation-GC/MS, and solid-state C-13 NMR. *Geochemistry, Geophysics, Geosystems* 14: 3176–3191.
- Woodroffe CD (1981) Mangrove swamp stratigraphy and Holocene transgression, Grand Cayman Island, West Indies. *Marine Geology* 41: 271–294.
- Woodroffe CD (1988a) Changing mangrove and wetland environments over the last 8000 years, northern Australia and south-east Asia. In: Wade-Marshall D and Loveday P (eds) *Northern Australia: Progress and Prospects, Volume 2: Floodplains Research*. Canberra: North Australia Research Unit, Australian National University, pp. 1–33.
- Woodroffe CD (1988b) Mangroves and sedimentation in reef environments: Indicators of past sea-level changes, and present sea-level trends? In: Choat JH, Barnes D, Borowitzka MA, et al. (eds) *Proceedings of the 6th International Coral Reef Symposium: Vol. 3. Contributed Papers*. Townsville, pp. 535–539.
- Woodroffe CD (1990) The impact of sea-level rise on mangrove shorelines. *Progress in Physical Geography* 14: 483–520.
- Woodroffe CD, Thom BG and Chappell J (1985) Development of widespread mangrove swamps in mid-Holocene times in Northern Australia. *Nature* 317: 711–713.
- Woodroffe SA (2009) Testing models of mid-late Holocene sea-level change, North Queensland, Australia. *Quaternary Science Reviews* 28: 2474–2488.
- Woodroffe SA (in preparation) New constraints on late Holocene eustatic sea-level changes from the Seychelles. *Quaternary Science Reviews*.
- Wooller MJ, Morgan R, Fowell S et al. (2007) A multiproxy peat record of Holocene mangrove palaeoecology from Twin Cays, Belize. *The Holocene* 17: 1129–1139.
- Zinke J, Reijmer JJG, Taviani M et al. (2005) Facies and faunal assemblage changes in response to the Holocene transgression in the Lagoon of Mayotte (Comoro Archipelago, SW Indian Ocean). *Facies* 50: 391–408.
- Zinke J, Reijmer JJG, Thomassin BA et al. (2003) Post-glacial flooding history of Mayotte lagoon (Comoro Archipelago, southwest Indian Ocean). *Marine Geology* 194: 181–196.